$Cr^{3+} \rightarrow Nd^{3+}$ energy transfer in fluorophosphate glass investigated by time-resolved laser spectroscopy

R. Balda and J. Fernández
Departamento de Física Aplicada I, Escuela Técnica Superior de Ingenieros Industriales y de Telecomunicación, Universidad del País Vasco, Alameda de Urquijo s/n 48013 Bilbao, Spain

A. de Pablos and J. M. Fernández-Navarro
Instituto de Cerámica y Vidrio, Arganda del Rey Madrid, Spain
(Received 19 November 1992; revised manuscript received 21 April 1993)

Energy transfer between chromium and neodymium ions in a mixed fluorophosphate glass [$21.74Al(PO_3)_3$-$57.8BaF_2$-16.96 AlF_3] has been investigated in the 4.2–300 K temperature range by using steady-state and time-resolved laser spectroscopy. Radiative and nonradiative energy transfer has been demonstrated from the time-resolved emission spectra and the decrease of the Cr^{3+} lifetimes. Comparison between time-resolved emission spectra for Cr^{3+} singly doped and codoped samples with different Nd^{3+} concentrations shows that the radiative transfer is linearly dependent on Nd^{3+} concentration. The nonradiative energy transfer is consistent with an electric-dipole–electric-dipole interaction mechanism. Good agreement is found if transfer efficiency corrected for Nd-Nd self-quenching is compared with the measured sensitized Nd^{3+} luminescence. The transfer efficiency of a Cr^{3+}, Nd^{3+} system in the investigated fluorophosphate glass has also been compared with previous results in a pure fluoride glass giving a higher efficiency for the fluorophosphate glass if the Nd_2O_3 concentration is kept below 2 wt %.

I. INTRODUCTION

Chromium ions have been added to rare-earth laser materials to sensitize the fluorescence and thereby increase the optical-pumping efficiency. Neodymium-doped glasses are by far the most widely investigated systems, and many of the observed luminescence features for Nd^{3+} ions are also applicable to other rare earths.[1] For Nd^{3+} ions, trivalent chromium is an attractive sensitizing ion because it has broad, strong absorption bands in the visible range and its emission is in the red and near-infrared region, where Nd^{3+} has strong absorption transitions. Efficient nonradiative energy transfer from Cr^{3+} to Nd^{3+} has been observed in various glasses.[2–7] In a previous work, some of the authors have investigated the optical properties of Cr^{3+} ions in fluorophosphate glass by using steady-state and time-resolved spectroscopy.[8] In this fluorophosphate glass the Cr^{3+} ions relax via a broadband fluorescence from the $^4T_2$ state. This emission is in the near infrared and overlaps the Nd^{3+} absorption; therefore efficient energy transfer could be expected.

The aim of this work is to describe the main features of Cr^{3+} to Nd^{3+} energy transfer in this fluorophosphate glass and to determine the transfer and luminescence efficiencies as a function of Nd^{3+} concentration and temperature. Radiative and nonradiative transfer are investigated using steady-state and time-resolved spectroscopy. The time-resolved emission spectra provide information about the radiative and nonradiative energy transfer whereas the fluorescence decay properties of Cr^{3+} ions in the presence of Nd^{3+} provide information about the rates and efficiencies of nonradiative energy transfer. The results of this investigation have been compared with previous results[7] in a pure fluoride glass (30 BaF_2-18lnF_3-12GaF_3-20ZnF_2-10YF_3-6ThF_3-4ZrF_3) paying attention to the influence of the mixed nature of the fluorophosphate glass on the Cr^{3+} to Nd^{3+} transfer efficiency as well as to the concentration self-quenching of Nd^{3+} fluorescence. If account is taken of both processes, for Nd_2O_3 concentrations below 2 wt %, the Nd^{3+} sensitized luminescence in the fluorophosphate glass is higher than in the pure fluoride glass.

II. EXPERIMENTAL TECHNIQUES

Fluorophosphate glass samples were obtained with the composition $21.74Al(PO_3)_3$-$57.8BaF_2$-$16.96AlF_3$ in wt % and doped with Cr_2O_3 and Nd_2O_3. The concentration of both dopants in wt % is given in Table I. The glasses were prepared by melting the precursor mixture in platinum crucibles in an electric furnace heated to 1200 °C un-

TABLE I. Dopant concentrations in wt % for the fluorophosphate glass.

Sample number	Cr_2O_3 (wt %)	Nd_2O_3 (wt %)
1	0.5	0
2	0	0.1
3	0	0.5
4	0	1
5	0	2
6	0	3
7	0	5
8	0.5	0.5
9	0.5	1
10	0.5	2
11	0.5	5

der a controlled atmosphere. Then the melt was poured into a brass mould and annealed at 500 °C. Finally, the samples were cut and polished for optical measurements.

The sample temperature was varied between 4.2 and 300 K with a continuous flow cryostat. Conventional absorption spectra were performed with a CARY 5 spectrophotometer. The emission measurements were made using the 633 nm emission line of a 15 mW He-Ne laser as exciting light, which was chopped at 200 Hz. The fluorescence was analyzed with a 0.22 m SPEX monochromator, and the signal was detected by a Hamamatsu R7102 extended IR photomultiplier and finally amplified by a standard lock-in technique. The system response was calibrated with a standard tungsten-halogen lamp which was calibrated as well against a National Bureau of Standards lamp, in order to correct the emission spectra.

Lifetime measurements were performed with a tunable dye laser (1 ns pulse width), pumped by a pulsed nitrogen laser. In order to describe the evolution of fluorescence, time-resolved spectroscopy has been used. The emission measurements were obtained by exciting the sample with a tunable dye laser and detecting the emission with a Hamamatsu R7102 photomultiplier. The spectra were processed by an EGG-Princeton Applied Research boxcar integrator.

III. SPECTROSCOPIC PROPERTIES OF Cr^{3+}

Before considering $Cr^{3+} \rightarrow Nd^{3+}$ energy transfer, the optical spectra and fluorescence kinetics of Cr^{3+} ions will be briefly reviewed. A more extensive presentation of the spectroscopic properties of Cr^{3+} ions was given by some of the authors in a separate paper.[8]

Figure 1(a) shows the room-temperature (RT) absorption spectrum of Cr^{3+} singly doped fluorophosphate glass. The absorption spectrum shows the typical broadbands, identified as the vibronically broadened transitions $^4A_2 \rightarrow {}^4T_2$ centered around 15 538 cm^{-1}, and $^4A_2 \rightarrow {}^4T_1$ around 22 522 cm^{-1}. The low-energy absorption band shows a fine structure due to the spin-forbidden $^4A_2 \rightarrow {}^2E$ and $^4A_2 \rightarrow {}^2T_1$ transitions. The assignment of this structure has been made following the Fano antiresonance interpretation.[8-10] The experimental energies of the absorption bands may be used to determine the strength Dq of the octahedral crystal field and the Racah parameters. The obtained Dq/B value shows that this glass provides low field sites for Cr^{3+} ions. As a consequence the emission is characterized by a broad and structureless band centered in the near infrared which corresponds to the $^4T_2 \rightarrow {}^4A_2$ transition. This emission shows a large Stokes shift and is strongly dependent on temperature. Table II contains a summary of spectroscopic data of Cr^{3+} in this glass. The crystal field parameters Dq and B were calcu-

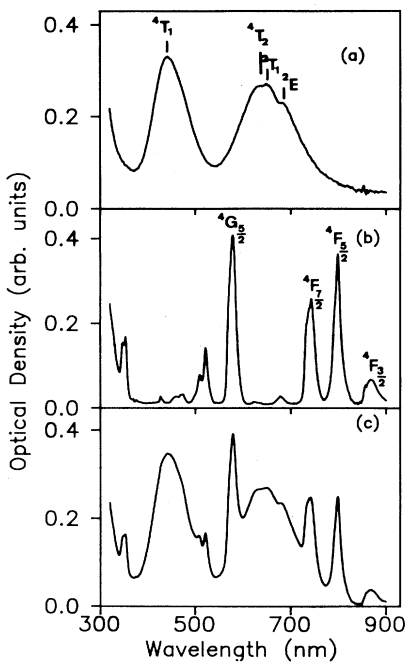

FIG. 1. Room-temperature absorption spectra of (a) Cr_2O_3 (0.5 wt %) singly doped glass, (b) Nd_2O_3 (2 wt %) singly doped glass, and (c) Cr_2O_3 (0.5 wt %), Nd_2O_3 (2 wt %) codoped glass.

lated using the Tanabe-Sugano matrix elements.[11] The $^4T_2$ emission peak position was used to determine a value of Dq/B for the relaxed excited state with the formula

$$\left[\frac{Dq}{B}\right]_{\mathrm{RES}} = \frac{E(^4T_2 \rightarrow {}^4A_2)}{10B} . \quad (1)$$

The time behavior of the Cr^{3+} fluorescence decay depends on the excitation, emission wavelength, and temperature. In addition, the decay is not single exponential at all temperatures and wavelengths. The best fit of the decay curves corresponds to a double-exponential function. The short-lived and long-lived components of the experimental decays obtained by a least squares fit are around 22 and 76 μs at liquid nitrogen temperature (LNT) for an emission wavelength of 880 nm.

The spectral dependence of the average lifetimes [defined by $\bar{\tau} = \int tI(t)dt / \int I(t)dt$] along the emission band is plotted in Fig. 2. As can be seen the lifetimes remain nearly constant at the shortest wavelength and then decrease as the wavelength increases. If a homogeneous site distribution were to be present, a monotonic dependence of lifetimes should be expected. These results are therefore consistent with a model of two or more sub-

TABLE II. Spectroscopic data of Cr^{3+} in fluorophosphate glass. Dq/B is the octahedral crystal field, $(Dq/B)_{\mathrm{RES}}$ is the crystal field for the relaxed excited state, ΔE_S is the Stokes shift, $h\nu_{\mathrm{em}}$ is the peak position of the $^4T_2 \rightarrow {}^4A_2$ transition, and σ is the half-width of the emission band.

	Dq/B	$(Dq/B)_{\mathrm{RES}}$	ΔE_S (cm^{-1})	$h\nu_{\mathrm{em}}$ (cm^{-1})	σ (cm^{-1})
LNT	2.16	1.58	4223	11 519	997
RT	2.12	1.6	3766	11 772	1101

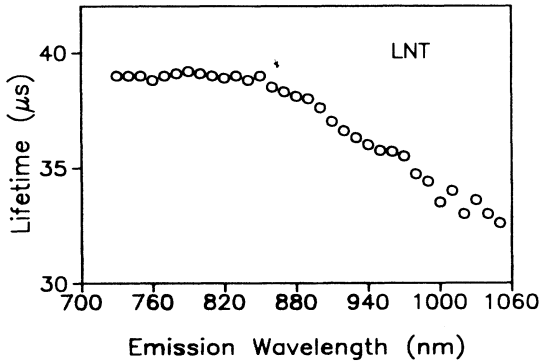

FIG. 2. LNT lifetimes at different emission wavelengths along the $^4T_2 \rightarrow {}^4A_2$ emission band for Cr^{3+} singly doped glass for an excitation wavelength of 655 nm. The data correspond to the average lifetime.

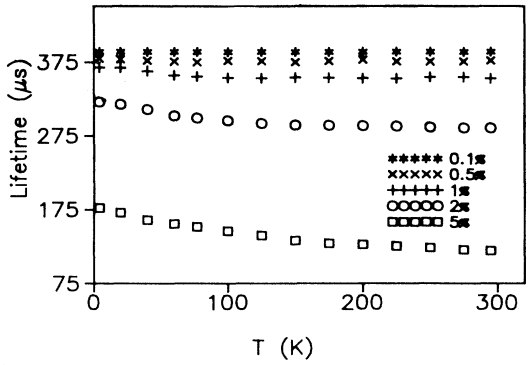

FIG. 3. Lifetimes as a function of temperature for singly doped Nd^{3+} glass with different concentrations (*) 0.1%, (×) 0.5%, (+) 1%, (○) 2%, and (□) 5%. Lifetimes were obtained by exciting at 575 nm and collecting the fluorescence at the emission peak of the $^4F_{3/2} \rightarrow {}^4I_{11/2}$ (1058 nm).

sets of Cr^{3+} ions with slightly different spectral dependences. The spectral dependence of the decays along the broad emission band, together with the results on time-resolved excitation and emission spectra, pointed out the existence of two statistical distributions for Cr^{3+} ions in fluorophosphate glass with a slightly different spectral dependence. If compared with the experimental results in fluoride glasses,[12–14] the mixed nature of the fluorophosphate glass seems to enhance the site-dependent effects.[8]

The Cr^{3+} emission in this glass shows a strong temperature dependence due to an increase of nonradiative transitions. The quantum efficiency at 300 K is low ($\approx 10\%$) in accordance with the strong thermal quenching of luminescence.[8]

IV. SPECTROSCOPIC PROPERTIES OF Nd^{3+}

The absorption spectra of Nd^{3+} singly doped fluorophosphate glass were obtained at 295 K in the 300–2500 nm spectral range. Figure 1(b) shows the absorption spectrum for the sample with 2 wt % of Nd_2O_3 in the 300–900 nm range of interest.

The absorption bands originating from the $^4I_{9/2}$ ground state were integrated, and these data, along with the values for the Nd^{3+} concentration and the refractive index were fitted by a computerized least squares program to yield the best fit values for the Judd[15]-Ofelt[16] (JO) parameters Ω_2, Ω_4, Ω_6. To estimate the JO parameters we have used the reduced matrix elements, $\|U^t\|^2$, reported by Carnall *et al.*[17] for Nd^{3+} ions in LaF_3. The values that were obtained ($\Omega_2 = 2.78 \times 10^{-20}$, $\Omega_4 = 4.24 \times 10^{-20}$, $\Omega_6 = 4.5 \times 10^{-20}$ cm^2) are in good agreement with those previously reported for the Nd^{3+} ion in different fluorophosphate glasses.[18–20]

The Ω_4 and Ω_6 parameters have been used to calculate the radiative parameters for the laser emission state $^4F_{3/2}$. The value of 402 μs was obtained for the radiative lifetime.

The decays of the $^4F_{3/2} \rightarrow {}^4I_{11/2}$ transition for the Nd_2O_3 concentrations (0.1, 0.5, 1, 2, and 5 wt %) were obtained under laser-pulsed excitation at the $^4I_{9/2} \rightarrow {}^4G_{5/2}$ absorption band (575 nm) as a function of temperature. These decays were found to be exponential for all temperatures and concentrations. The lifetime values as a function of temperature between 4.2 K and 300 K are presented in Fig. 3. The ratio of these experimental lifetimes and the radiative lifetime yields the calculated radiative quantum efficiency. At low concentration and temperature the measured lifetimes approach the predicted purely radiative rate. As the concentration rises the lifetimes remain exponential but a decrease in the experimental lifetime is observed even at helium temperature. As can be seen from Fig. 3, quenching of the Nd^{3+} fluorescence by $Nd^{3+} \rightarrow Nd^{3+}$ interactions is already present at concentrations higher than 1 wt %; any further addition of Nd^{3+} shortens the lifetime and reduces the quantum efficiency even at low temperatures. Figure 4 shows the decay rates of 0.1, 0.5, 1, 2, 3, and 5 wt % samples at three different temperatures (room, nitrogen, and helium temperatures). In this concentration range the effective decay rates show a linear dependence on the square of Nd_2O_3 concentration, indicating that $Nd^{3+} \rightarrow Nd^{3+}$ energy transfer probably occurs in the framework of a limited-diffusion regime.[21,22] The

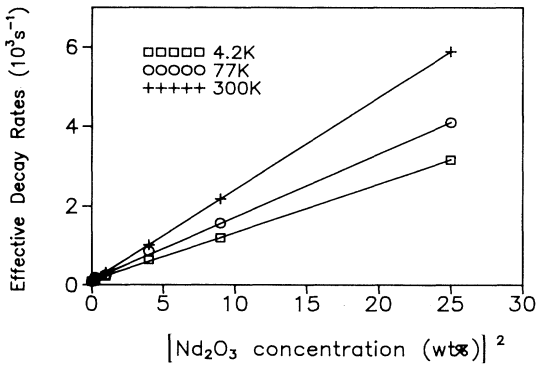

FIG. 4. Effective decay rates of singly doped Nd^{3+} fluorophosphate glass as a function of the square of Nd_2O_3 concentration at different temperatures: (□) 4.2 K, (○) 77 K, and (+) 300 K.

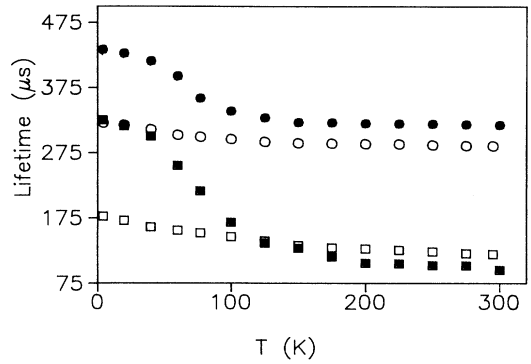

FIG. 5. Lifetimes as a function of temperature for singly doped Nd^{3+} pure fluoride glass (solid dots) and fluorophosphate glass (open dots) with different Nd concentrations (●) 4.3×10^{20} cm^{-3} (2 mol% NdF_3), (■) 10.8×10^{20} cm^{-3} (5 mol% NdF_3), (○) 3×10^{20} cm^{-3} (2 wt% Nd_2O_3), and (□) 7.6×10^{20} cm^{-3} (5 wt% Nd_2O_3). Lifetimes were obtained by exciting at 575 nm and collecting the fluorescence at the emission peak of the $^4F_{3/2}\rightarrow{}^4I_{11/2}$ (1058 nm). Data for the fluoride glass correspond to Ref. 7.

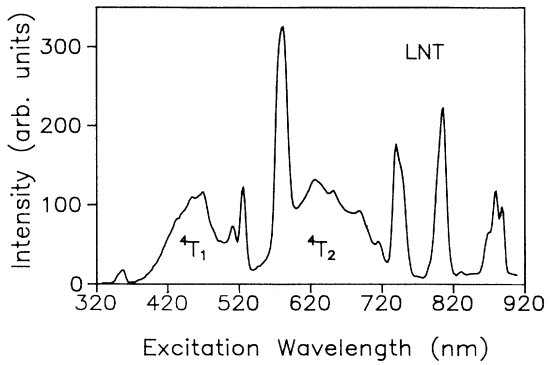

FIG. 6. LNT excitation spectrum of the Nd^{3+} fluorescence at 1058 nm for the codoped sample with 0.5% of Cr_2O_3 and 2% of Nd_2O_3. The spectrum is not corrected for variations in the source intensity.

diffusion is, however, fast enough to give exponential fluorescence decays.

As is well known the Nd^{3+} fluorescence quenching depends on glass composition.[23] For this mixed fluorophosphate glass we could expect an intermediate behavior between a pure phosphate and a pure fluoride. In a recent work some of the authors have found a nearly linear concentration dependence (at low temperature) for the Nd^{3+} luminescence in a pure fluoride glass.[7] For comparison Fig. 5 shows the thermal quenching of Nd^{3+} fluorescence in the pure fluoride glass and in the investigated fluorophosphate glass for several concentrations. As can be seen in spite of the strong concentration quenching of the fluorophosphate glass at low temperatures it has a weak temperature dependence. On the contrary the pure fluoride glass[7] has a strong thermal quenching between 15 K and 100 K where the nonradiative rates were found to increase with temperature as T^3. On the other hand, generally, a pure phosphate glass does not show a strong concentration quenching, its rate normally increases as the square of Nd^{3+} concentration.[23] Under these considerations we could conclude that in spite of its high fluoride content, our fluorophosphate glass shows a behavior which is close to a typical phosphate glass.

V. $Cr^{3+}\rightarrow Nd^{3+}$ ENERGY TRANSFER

The RT absorption spectrum of codoped sample for Cr_2O_3 and Nd_2O_3 concentrations of 0.5% and 2%, respectively, is shown in Fig. 1(c). The spectrum shows the narrow Nd^{3+} transitions superimposed to the broad absorption bands of Cr^{3+}.

The LNT excitation spectrum of the Nd^{3+} luminescence at 1058 nm for the codoped sample with 0.5% of Cr_2O_3 and 2% of Nd_2O_3 is shown in Fig. 6. A high-pressure xenon lamp and a 0.25 m grating monochromator were used. The presence of the broad $^4A_2\rightarrow{}^4T_1$ and $^4A_2\rightarrow{}^4T_2$ bands of Cr^{3+} besides the Nd^{3+} lines clearly indicates that a Cr^{3+} to Nd^{3+} energy transfer takes place.

Characteristic decays of the codoped glass were obtained under laser-pulsed excitation at the center of the $^4A_2\rightarrow{}^4T_2$ absorption band (655 nm) of Cr^{3+} as a function of temperature at two different emission wavelengths for all codoped samples. The lifetimes for Cr^{3+} were measured at 820 nm, and for Nd^{3+} the emission was monitored at 1058 nm. The time-dependent behavior of the Cr^{3+} fluorescence from the codoped samples at 77 K is shown in Fig. 7. This emission originated from the $^4T_2$ level of Cr^{3+} exhibited a multiexponential behavior, and a shortening of the lifetime as compared with the singly doped glass, because of the additional probability for relaxation by nonradiative energy transfer to Nd^{3+}. The decays obtained at the 1058 nm Nd^{3+} emission by exciting the Cr^{3+} ions into the $^4A_2\rightarrow{}^4T_2$ absorption band (655 nm) are exponential in all cases and the lifetimes decrease as the Nd^{3+} concentration increases.

The fluorescence decays for the 820 and 1058 nm emission were also measured in the 4.2 K–300 K temperature range. The values of the Cr^{3+} emission lifetimes, moni-

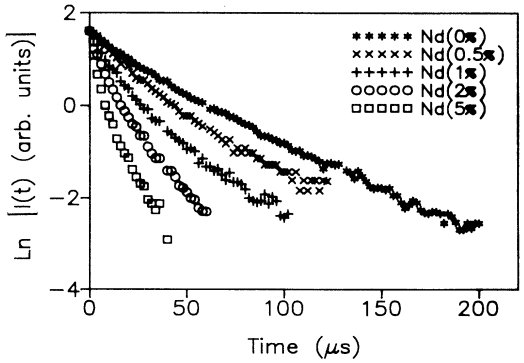

FIG. 7. Logarithmic plot of the fluorescence decays of the $^4T_2\rightarrow{}^4A_2$ emission monitored at 820 nm, in the codoped glass with different Nd_2O_3 concentrations, including zero, for an excitation wavelength of 655 nm. Measurements correspond to 77 K.

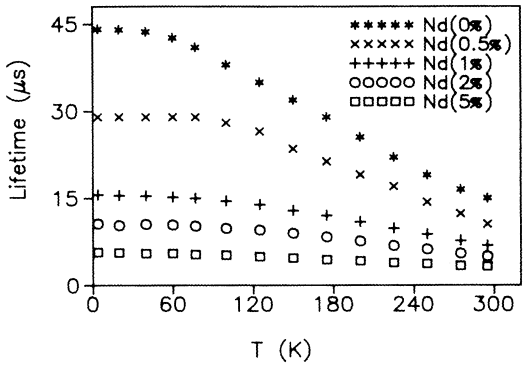

FIG. 8. Lifetimes of the Cr^{3+} emission as a function of temperature in Cr^{3+} singly doped glass (*) and in the codoped samples with different Nd_2O_3 concentrations: (×) 0.5%, (+) 1%, (○) 2%, and (□) 5%. Lifetimes were obtained by exciting at the center of the $^4A_2 \rightarrow {}^4T_2$ absorption band (655 nm) and collecting the fluorescence at 820 nm.

tored at 820 nm are shown in Fig. 8, which also includes the lifetime of singly doped glass for comparison. The Nd^{3+} decays, obtained by exciting the Cr^{3+} ions into the $^4A_2 \rightarrow {}^4T_2$ absorption band (655 nm), as a function of temperature for all codoped samples are presented in Fig. 9. As can be seen from this figure the lifetimes decrease as Nd^{3+} concentration and temperature increase.

A. Time-resolved emission spectra

The time-resolved (TR) emission spectra of Cr^{3+} singly doped and codoped glasses were obtained at liquid nitrogen temperature at different time delays after the pulsing laser. Figure 10 presents the TR emission spectra for the sample with 0.5% of Cr_2O_3 and 2% of Nd_2O_3 at different time delays ranging from 1 to 150 μs (gate widths ranging from 20 to 500 ns). The spectra are vertically shifted for better visualization and are scaled to have a similar height. These spectra show, superimposed to the Cr^{3+} emission, the Nd^{3+} emission around 900 and 1058 nm,

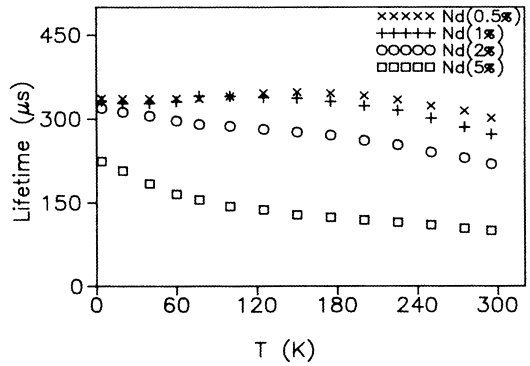

FIG. 9. Lifetimes as a function of temperature for all codoped samples with different Nd_2O_3 concentrations: (×) 0.5%, (+) 1%, (○) 2%, and (□) 5%. Lifetimes were obtained by exciting at the center of the $^4A_2 \rightarrow {}^4T_2$ absorption band (655 nm) and collecting at the emission peak of the $^4F_{3/2} \rightarrow {}^4I_{11/2}$ transition.

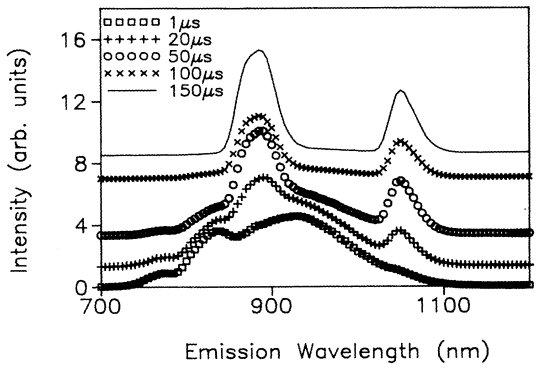

FIG. 10. Time-resolved emission spectra taken at different time delays (between 1 and 150 μs) for the codoped glass with 2% of Nd_2O_3. The spectra are scaled and vertically shifted for better visualization. Measurements were performed at 77 K, for an excitation wavelength of 655 nm.

and two dips around 800 and 870 nm due to radiative absorption by Nd^{3+} absorption bands in this spectral range. These results show that even at quite a short time, radiative and nonradiative energy transfer to Nd^{3+} exists. As can be seen from this figure, at short times after pulsing, both Cr^{3+} and Nd^{3+} emissions are observed, but at 150 μs the emission spectrum mainly consists of Nd^{3+} bands, since Cr^{3+} ions initially excited have already decayed (lifetime ≈15 μs) and only long-lived Nd^{3+} ions (lifetime

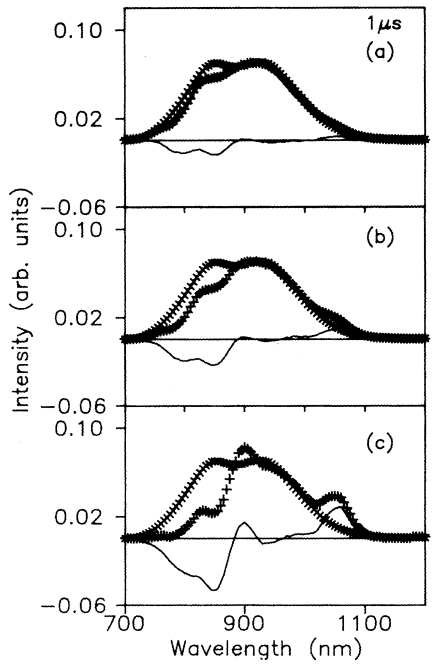

FIG. 11. Comparison between (×) scaled time-resolved emission spectrum of $^4T_2 \rightarrow {}^4A_2$ transition in singly doped Cr^{3+} glass, and (+) time-resolved emission spectrum of the codoped samples with different Nd_2O_3 concentrations obtained at 1 μs time delays. (a) Nd_2O_3 (1 wt %), (b) Nd_2O_3 (2 wt %), (c) Nd_2O_3 (5 wt %). The difference between both spectra is represented by a solid line. The spectra were obtained by exciting at 655 nm. Measurements were performed at 77 K.

$\approx 300\ \mu s$) make a contribution to the emission spectrum.

The presence of nonradiative $Cr^{3+} \rightarrow Nd^{3+}$ energy transfer was determined by observing the increased decay rate of the Cr^{3+} fluorescence with increasing Nd^{3+} concentration. It was also evident that together with a nonradiative transfer, a radiative $Cr^{3+} \rightarrow Nd^{3+}$ energy transfer involving the emission of Cr^{3+} photons and subsequent absorption by Nd^{3+} ions exists, as shown by the dips in the TR emission spectra (see Fig. 10). In order to make a qualitative estimate of this radiative contribution and establish time-scale limits for the energy transfer, very careful time-resolved emission spectra were performed at 100 ns, 500 ns, and 1 μs time delays, exciting the Cr^{3+} ions in three codoped samples (Cr_2O_3 0.5%, Nd_2O_3 1%, 2%, and 5%). Since only the qualitative comparison between emission spectra was of interest, no corrections were made for the spectral response of the system. As an example Fig. 11 shows these spectra normalized with the one obtained for the Cr^{3+} singly doped glass at 1 μs time delay. As can be seen from this figure the subtraction between the scaled TR emission spectra of Cr^{3+} singly doped glass and the TR emission of codoped samples shows the two Nd^{3+} emissions at 900 and 1058 nm and the Nd^{3+} absorptions corresponding to the dips observed around 800 and 870 nm. From these results, some conclusions can be inferred: (i) As theoretically predicted, the radiative contribution to the transfer represented by the dips in the emission spectra shows a linear dependence on Nd^{3+} concentration. (ii) As time and Nd^{3+} concentration increase, the luminescence from the $^4F_{3/2} \rightarrow {}^4I_{11/2}, I_{9/2}$ is enhanced as can be seen on the upper side of the base line showing that an effective transfer occurs. (iii) $Cr^{3+} \rightarrow Nd^{3+}$ transfer is already present below 100 ns, corresponding to transfer rates higher than $10^7\ s^{-1}$ which are faster than nonradiative relaxation of Cr^{3+} in the singly doped glass ($\approx 10^4\ s^{-1}$).

The presence of nonradiative $Cr^{3+} \rightarrow Nd^{3+}$ energy transfer can be demonstrated by the time-dependent behavior of the Cr^{3+} fluorescence from the codoped samples. Figure 7 showed an increasing rate for the Cr^{3+} decays as a function of Nd^{3+} concentration due to the additional nonradiative relaxation probabilities. On the other hand, the Cr^{3+} emission from the $^4T_2$ level of a chromium singly doped glass shows an intrinsic double-exponential behavior, which can be related with the existence of slightly different statistical distributions of Cr^{3+} ion environments. As energy transfer can be excluded between donors[8] only a direct energy transfer to acceptors can affect the Cr^{3+} lifetime at a given temperature. For this type of donor-acceptor system the fluorescence decay has been theoretically studied by Inokuti-Hirayama under the assumption that energy transfer processes result from electric multipole interactions.[24]

According to the Inokuti-Hirayama model,[25] if higher-order processes can be neglected, the normalized donor decay curves can be expressed by

$$\Phi(t)=\exp\left[-\frac{t}{\tau_0}-\frac{4}{3}\pi\Gamma\left(1-\frac{3}{s}\right)N_i R_0^3\left(\frac{t}{\tau_0}\right)^{3/s}\right] \quad (2)$$

with $S=6$, 8, and 10, respectively, for electric dipole-dipole, dipole-quadrupole, and quadrupole-quadrupole interactions. N_i is the acceptor concentration and R_0 is the critical transfer distance defined as the one for which the probability for energy transfer between a given donor-acceptor pair is equal to the donor intrinsic decay probability τ_0^{-1}. To determine the appropriate multipole interaction we have analyzed the measured Cr^{3+} decay curves with respect to Eq. (2). Although it is difficult to know the exact multipolar nature of the $Cr^{3+} \rightarrow Nd^{3+}$ transfer process we have found that a dipole-dipole transfer is consistent with the experimental decay intensities if account is taken of the short- and long-lived components of the Cr^{3+} intrinsic lifetimes.[26] Figure 12(a) shows a least square fit of the experimental Cr^{3+} decay at LNT of a codoped sample with Nd_2O_3 (1 wt %) to Eq. (2) using the Cr^{3+} intrinsic average lifetime τ_0. The obtained value for R_0 was 9.6 ± 1 Å. Figure 12(b) gives the fitting to the linear combination $\lambda_1\Phi(t,\tau_0^l)+\lambda_2\Phi(t,\tau_0^s)$ based on Eq. (2) using the values of τ_0 belonging to the short-lived (s) and long-lived (l) components of the intrinsic Cr^{3+} decays. In this last case a best fit is obtained giving to the mean critical transfer distance a value of 8 Å.

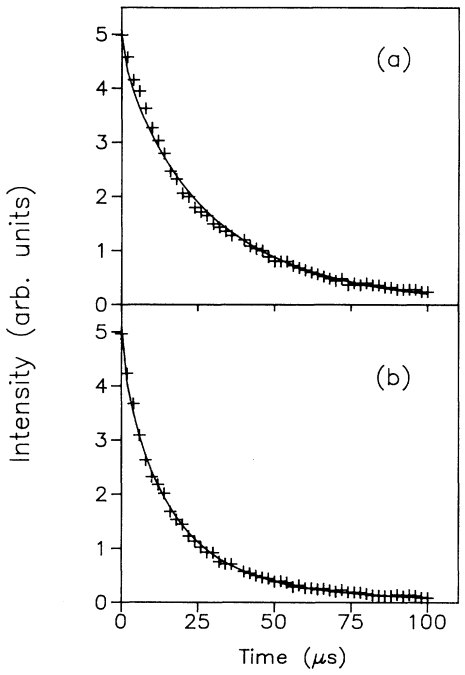

FIG. 12. Cr^{3+} emission showing the fitting between the experimental decay curves (+) and the calculated ones for dipole-dipole interaction ($s=6$) (solid lines) for the codoped sample with 1 wt % of Nd_2O_3: (a) using the average lifetime of Cr^{3+} at 820 nm, and (b) using the short-lived and long-lived components of the Cr^{3+} decay. Measurements correspond to 77 K.

B. Transfer efficiency

The transfer efficiency was estimated according to the expression

$$\eta_t(\tau)=1-\frac{\tau}{\tau_0},$$

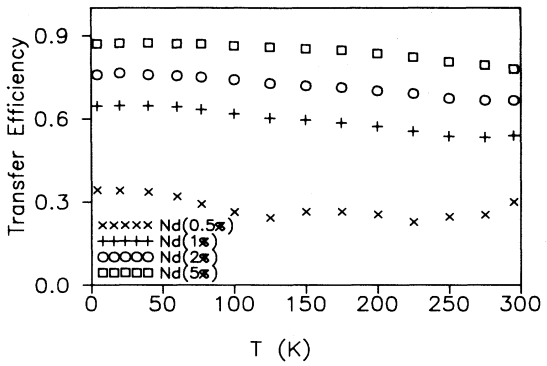

FIG. 13. Transfer efficiency as a function of temperature for an emission wavelength of 820 nm, in codoped samples. (×) 0.5%, (+) 1%, (○) 2%, and (□) 5%.

with τ and τ_0 being the Cr^{3+} mean decay times monitored at 820 nm, with and without Nd^{3+} ions. Figure 13 shows the transfer efficiencies for the codoped samples as a function of temperature. As can be seen this transfer efficiency presents a weak dependence on temperature. Figure 14 gives the Cr^{3+} to Nd^{3+} transfer efficiency and the estimated quantum efficiency of the Nd^{3+} emission as a function of Nd^{3+} concentration at 300 K. As can be seen, transfer becomes quite efficient at high Nd^{3+} concentrations. However, because of the strong luminescence quenching of Nd^{3+} with concentration (see Sec. IV) it is obvious that a compromise should be reached for maximizing the sensitized luminescence emitted by Nd^{3+}. In order to analyze this point, Nd^{3+} luminescence emission measurements were performed on the codoped samples in such a way that an absolute comparison could be made among different Nd^{3+} concentrations. The experimental procedure was the one followed in Ref. 7. The recorded fluorescence of the measured samples normalized to the 2% Nd_2O_3 sample is given in Fig. 15. As can be observed this sample has the highest luminescence efficiency. In spite of this, the highest theoretical efficiency, calculated by using the values of the $Cr^{3+} \rightarrow Nd^{3+}$ transfer efficiency and the quantum

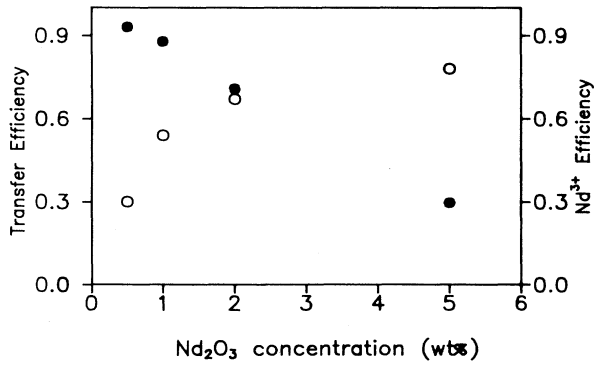

FIG. 14. $Cr^{3+} \rightarrow Nd^{3+}$ transfer efficiency calculated for an emission wavelength of 820 nm (○), and Nd^{3+} estimated quantum efficiency (●) vs Nd_2O_3 concentration in the codoped samples. Data correspond to 300 K.

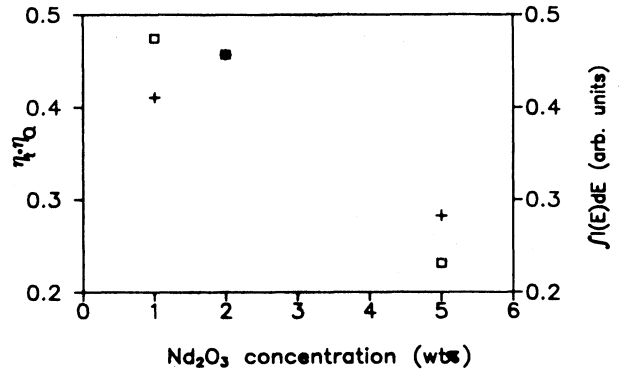

FIG. 15. Integrated emission intensities of the $^4F_{3/2} \rightarrow {}^4I_{11/2}$ transition (+), and theoretical efficiency $\eta = \eta_t \eta_Q$ (□), calculated by using the values of the transfer efficiency η_t and the quantum efficiency η_Q of the Nd^{3+} emission, as a function of Nd_2O_3 concentration for the three codoped samples.

efficiency of the Nd^{3+} emission, corresponds to the 1% sample. This disagreement ($\approx 10\%$) is not surprising considering the inherent errors in the measurements.

In order to compare the $Cr^{3+} \rightarrow Nd^{3+}$ transfer efficiency in a pure fluoride glass[7] and in the fluorophosphate glass under study, Fig. 16 shows the theoretical efficiency calculated by using the values of the transfer efficiency and the quantum efficiency of the Nd^{3+} emission as a function of Nd^{3+} concentration. As can be observed, at low Nd^{3+} concentration fluorophosphate glass shows the highest efficiency. Nevertheless, as concentration increases the Nd^{3+} self-quenching governs the transfer process and the efficiency of fluorophosphate glass is significantly reduced.

VI. CONCLUSIONS

(i) Cr^{3+} to Nd^{3+} radiative and nonradiative energy transfer has been demonstrated from the time-resolved emission spectra and the decrease of the Cr^{3+} fluores-

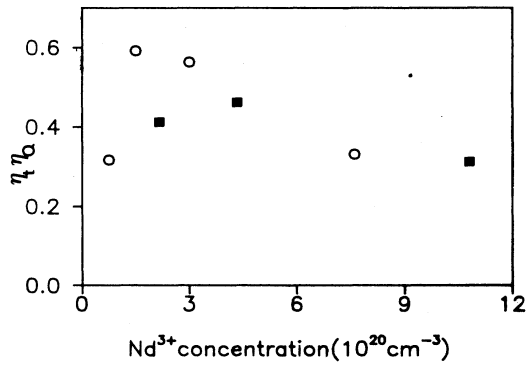

FIG. 16. Theoretical efficiency $\eta = \eta_t \eta_Q$, calculated by using the values of the transfer efficiency η_t and the quantum efficiency η_Q of the Nd^{3+} emission, as a function of Nd^{3+} concentration (at 77 K) for the fluorophosphate glass (○) and for a pure fluoride glass (□). Data for the fluoride glass correspond to Ref. 7.

cence lifetime. The comparison between time-resolved emission spectra from Cr^{3+} singly doped and codoped samples allows us to evaluate the contribution of radiative energy transfer which shows a linear dependence on Nd^{3+} concentration.

(ii) Although it is difficult to establish the exact multipolar nature of the $Cr^{3+} \rightarrow Nd^{3+}$ transfer process, dipole-dipole transfer is consistent with the experimental decay intensities if account is taken of the short- and long-lived components of the Cr^{3+} intrinsic lifetime.

(iii) Transfer efficiency, which has been studied as a function of acceptor concentration and temperature, reaches 78% at room temperature for the highest Nd^{3+} concentration.

(iv) Nd^{3+} luminescence emission measurements in the codoped samples have been performed in such a way that an absolute comparison could be made among different Nd^{3+} concentrations. The codoped sample with 2% of Nd_2O_3 shows the best luminescence efficiency. In spite of this, the highest theoretical efficiency, calculated by using the values of the $Cr^{3+} \rightarrow Nd^{3+}$ transfer efficiency and the quantum efficiency of the Nd^{3+} emission, corresponds to the 1% sample.

(v) The transfer efficiency corrected for the Nd-Nd self quenching is higher than in pure fluoride glass for Nd_2O_3 concentrations below 2 wt %.

ACKNOWLEDGMENTS

This work was supported by the Comisión Interministerial de Ciencia y Tecnología (CICYT) of the Spanish Government (Ref. 0434/93), Basque Country Government (Ref. PGV 9012), and Basque Country University (Ref. E126/91).

[1]M. J. Weber, J. Non-Cryst. Solids **123**, 208 (1990).
[2]R. Reisfeld, in *Energy Transfer Processes in Condensed Matter,* edited by B. Di Bartolo (Plenum, New York, 1984), p. 521.
[3]J. G. Edwards and S. Gomulka, J. Phys. D **12**, 187 (1979).
[4]A. G. Avasenov *et al.*, Kvant. Elektron. (Moscow) **6**, 1538 (1979) [Sov. J. Quantum Electron. **9**, 935 (1979)].
[5]T. Härig, G. Huber, and I. A. Shcherbakov, J. Appl. Phys. **52**, 4450 (1981).
[6]A. Van Die, A. J. Faber, G. Blasse, and W. F. Van Der Weg, J. Phys. Chem. Solids **47**, 1081 (1986).
[7]M. J. Elejalde, R. Balda, J. Fernández, E. Macho, and J. L. Adam, Phys. Rev. B **46**, 5169 (1992).
[8]R. Balda, J. Fernández, and M. A. Illarramendi, J. Phys. Condens. Matter **4**, 10 323 (1992).
[9]U. Fano, Phys. Rev. **124**, 1866 (1961).
[10]U. Fano and J. W. Cooper, Phys. Rev. **137**, A1364 (1965).
[11]S. Sugano, Y. Tanabe, and H. Kamimura, *Multiplets of Transition-Metal Ions in Crystals* (Academic, New York, 1970).
[12]R. Balda, J. Fernández, M. A. Illarramendi, M. A. Arriandiaga, J. L. Adam, and J. Lucas, Phys. Rev. B **44**, 4759 (1991).
[13]M. A. Illarramendi, J. Fernández, R. Balda, J. Lucas, and J. L. Adam, J. Lumin. **47**, 207 (1991).
[14]R. Balda, J. Fernández, M. J. Elejalde, M. A. Illarramendi, and C. Jacoboni, J. Phys. Condens. Matter **3**, 7695 (1991).
[15]B. R. Judd, Phys. Rev. **127**, 750 (1962).
[16]G. S. Ofelt, J. Chem. Phys. **377**, 511 (1962).
[17]W. T. Carnall, P. R. Fields, and K. Rajnak, J. Chem. Phys. **49**, 4424 (1968).
[18]R. R. Jacobs and M. J. Weber, IEEE J. Quantum Electron. **QE-12**, 102 (1976).
[19]C. Brecher, L. A. Riseberg, and M. J. Weber, Phys. Rev. B **18**, 5799 (1978).
[20]A. Tesar, J. Campbell, and M. J. Weber, Opt. Mater. **1**, 217 (1992).
[21]M. J. Weber, Phys. Rev. B **4**, 2932 (1971).
[22]B. Henderson and G. Imbusch, *Optical Spectroscopy of Inorganic Solids* (Oxford University Press, Oxford, 1989), Chap. 10.
[23]S. E. Stokowski, in *Laser, Spectroscopy and New Ideas,* edited by W. M. Yen and M. D. Levensen (Springer-Verlag, Berlin, 1987), p. 47.
[24]W. Lenth, G. Huber, and D. Fay, Phys. Rev. B **23**, 3877 (1981).
[25]M. Inokuti and F. Hirayama, J. Chem. Phys. **43**, 1978 (1965).
[26]A similar procedure was developed by some of the authors for the case of $Cr^{3+} \rightarrow Nd^{3+}$ energy transfer in a pure fluoride glass in Ref. 7.